# Controlling Electrons and Protons through Theory: Molecular Electrocatalysts to Nanoparticles

Sharon Hammes-Schiffer

*Department of Chemistry, Yale University, 225 Prospect Street, New Haven, Connecticut 06520*

e-mail: sharon.hammes-schiffer@yale.edu

**Conspectus**

The development of renewable energy sources that are environmentally friendly and economical is of critical importance. The effective utilization of such energy sources relies on catalysts to facilitate the interconversion between electrical and chemical energy through multi-electron, multi-proton reactions. The design of effective catalysts for these types of energy conversion processes requires the ability to control the localization and movement of electrons and protons, as well as the coupling between them. Theoretical calculations, in conjunction with experimental validation and feedback, are playing a key role in these catalyst design efforts. A general theory has been developed for describing proton-coupled electron transfer (PCET) reactions, which encompass all reactions involving the coupled transfer of electrons and protons, including sequential and concerted mechanisms for multi-electron, multi-proton processes. In addition, computational methods have been devised to compute the input quantities for the PCET rate constant expressions and to generate free energy pathways for molecular electrocatalysts. These methods have been extended to heterogeneous PCET reactions to enable the modeling of PCET processes at electrode and nanoparticle surfaces.

Three distinct theoretical studies of PCET reactions relevant to catalyst design for energy conversion processes are discussed. In the first application, theoretical calculations of hydrogen production catalyzed by hangman metalloporphyrins predicted that the porphyrin ligand is reduced, leading to dearomatization and proton transfer from the carboxylic acid hanging group to the *meso* carbon of the porphyrin rather than the metal center, producing a phlorin intermediate. Subsequent experiments isolated and characterized the phlorin intermediate, validating this theoretical prediction. These molecular electrocatalysts exemplify the potential use of non-innocent ligands to localize electrons and protons on different parts of the catalyst and to direct

their motions accordingly. In the second application, theoretical calculations on substituted benzimidazole phenol molecules predicted that certain substituents would lead to multiple intramolecular proton transfer reactions upon oxidation. Subsequent experiments verified these multi-proton reactions, as well as the predicted shifts in the redox potentials and kinetic isotope effects. These bioinspired molecular systems demonstrate the potential use of multi-proton relays to enable the transport of protons over longer distances along specified pathways, as well as the tuning of redox potentials through this movement of positive charge. In the third application, theoretical studies of heterogeneous PCET in photoreduced ZnO nanoparticles illustrated the significance of proton diffusion through the bulk of the nanoparticle as well as interfacial PCET to an organic radical in solution at its surface. These theoretical calculations were consistent with prior experimental studies of this system, although theoretical methods for heterogeneous PCET have not yet attained the level of predictive capability highlighted for the molecular electrocatalysts. These examples suggest that theory will play a significant role in the design of both molecular and heterogeneous catalysts to control the movement and coupling of electrons and protons. The resulting catalysts will be essential for the development of renewable energy sources to address current energy challenges.

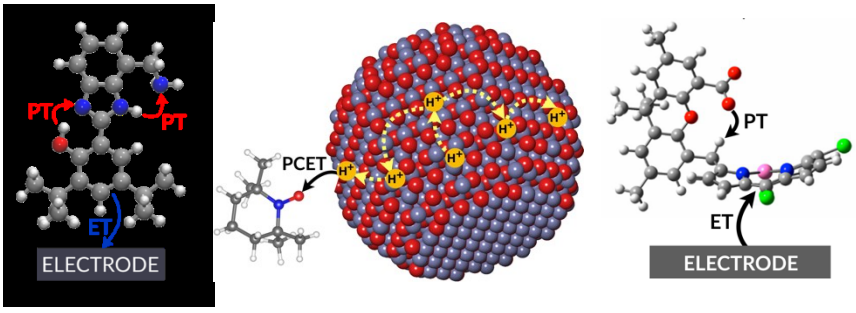

## Introduction

The effective utilization of renewable energy sources such as solar or wind requires the interconversion between electrical energy and fuels, which store energy in the form of chemical bonds. This interconversion process is facilitated by catalysts that are designed to control multi-electron, multi-proton reactions, such as the splitting of water into molecular hydrogen and oxygen.[1-5] As a result, significant attention has been directed toward the design of catalysts that are able to control the movement of electrons and protons, as well as the coupling between them. The objective of such catalyst design efforts is to control the localization of the electrons and protons where and when they are needed during the catalytic process. To accomplish this level of control, the catalysts should be designed to transfer electrons and protons in specified directions to targeted sites in a predetermined coupled or uncoupled manner.

The general term for reactions involving the coupled transfer of electrons and protons is proton-coupled electron transfer (PCET).[6-13] Although the simplest type of PCET reaction consists of a single electron transfer (ET) and a single proton transfer (PT) reaction, the term also applies to multi-electron, multi-proton reactions. Moreover, PCET also encompasses both sequential mechanisms, which exhibit stable intermediates, and concerted mechanisms, which exhibit the simultaneous transfer of an electron and a proton without a stable intermediate. These distinctions are not always well-defined, however, because the observation of a stable intermediate may depend on its lifetime, the experimental technique, or the level of theory. Although a sequential mechanism is definitively proven if an intermediate is observed, the confirmation of a concerted mechanism can be more challenging. Often thermodynamic considerations provide a strong indication of a concerted mechanism because the intermediate arising from a sequential mechanism would be thermodynamically unfavorable (i.e., significantly uphill in free energy).

However, even in the absence of a stable intermediate, a concerted PCET reaction could be asynchronous, especially considering the delocalization of electrons and protons. Furthermore, multi-electron, multi-proton processes could involve a combination of concerted and sequential steps.

Over the past two decades, we have been developing a PCET theory that encompasses all of these possibilities within a general framework.[6,9,12,14-17] In this Account, we start by summarizing the key concepts underlying this PCET theory, as well as the methods developed to compute the properties that enable the generation of thermodynamic pathways for molecular electrocatalysts and the input quantities for the PCET rate constant expressions. After this brief overview of PCET theory, we discuss three applications relevant to catalyst design for energy conversion processes. The first application focuses on hangman metalloporphyrins and illustrates the design of molecular electrocatalysts with non-innocent ligands that can be reduced and/or protonated.[18-19] The second application centers on the design of multi-proton relays, where oxidation of a substituted benzimidazole phenol (BIP) molecule is accompanied by multiple intramolecular proton transfer reactions, allowing the net transport of protons over longer distances.[20] The third application represents an example of heterogeneous PCET in nanoparticles, highlighting the significance of proton diffusion through the bulk of the nanoparticle as well as PCET at its surface.[21-22] The first two applications illustrate the predictive power of theory, and all three applications highlight the importance of feedback between theory and experiment in catalyst design.

**PCET Theory and Computation**

Our general PCET theory describes a PCET reaction in terms of $2^N$ diabatic states corresponding to the $N$ possible ET and PT reactions.[14] Thus, a reaction involving one ET and one PT reaction ($N = 2$) is described in terms of four diabatic states, while a reaction involving one ET and two PT reactions ($N = 3$) is described in terms of eight diabatic states. This framework allows the description of both sequential and concerted mechanisms, according to the definitions discussed in the Introduction. Various terminologies have been used in the literature to describe concerted PCET reactions. In this Account, a concerted mechanism involving the transfer of one electron and one proton is denoted EPT, while a concerted mechanism involving the transfer of one electron and two protons is denoted E2PT.

In this PCET theory,[6,9,12,14-17] the electrons and transferring proton(s) are treated quantum mechanically. Analogous to Marcus theory for electron transfer,[23] the free energy curves for the diabatic states can be expressed as functions of a collective solvent coordinate (Figure 1), but in this case these free energy curves correspond to mixed electron-proton vibronic states rather than purely electronic states. The PCET reaction is described in terms of nonadiabatic transitions between reactant and product electron-proton vibronic states. Within this framework, we have derived rate constant expressions in various well-defined regimes.[15-16,24] Typically the types of PCET reactions described herein are nonadiabatic due to small vibronic coupling. In this case, the vibronically nonadiabatic rate constant expression consists of a summation over pairs of reactant and product electron-proton vibronic states.[15] Each term in the summation depends exponentially on a free energy barrier, which is expressed in terms of the reaction free energy $\Delta G^{o}$ and reorganization energy $\lambda$ (Figure 1), and is proportional to the square of the vibronic coupling, which is typically expressed as the product of an electronic coupling and the overlap integral

between the reactant and product proton vibrational wavefunctions. Because this overlap integral depends strongly on the proton donor-acceptor distance, the proton donor-acceptor motion is also incorporated into the rate constant expressions.[16,24] These rate constant expressions have been applied to a wide range of PCET reactions and have been shown to reproduce experimentally measured relative rate constants and kinetic isotope effects (i.e., the ratio of the rate constants for hydrogen and deuterium).

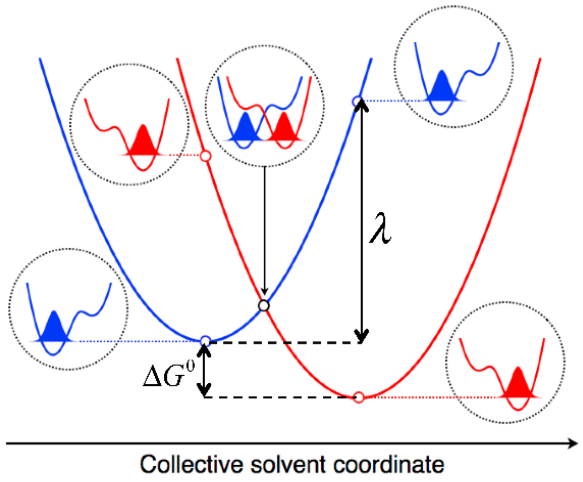


**Figure 1:** Free energy curves for the ground reactant (blue) and product (red) diabatic electron-proton vibronic states along the collective solvent coordinate for an EPT reaction. The proton potential energy curves along the proton coordinate and the corresponding ground state proton vibrational wavefunctions are depicted for open circle points on the free energy curves. Adapted with permission from Ref. 9. Copyright 2008 American Chemical Society.

We have also developed computational methods to compute the input quantities to these PCET rate constant expressions. For this purpose, as well as to facilitate theoretical studies of molecular electrocatalysts, we have developed a computational protocol for calculating reduction potentials and p$K_a$ values.[25] In this protocol, the reaction free energies are computed with density functional theory (DFT) combined with a polarizable continuum model to include solvent effects. The reduction potentials and p$K_a$ values are calculated relative to a related reference reaction for

which the quantity is known experimentally. This protocol has been benchmarked extensively by comparison to experimental data for many different types of molecular electrocatalysts. Similar methods are used to compute reaction free energies for concerted PCET reactions. In addition, we have developed methods for calculating inner-sphere (solute) and outer-sphere (solvent) reorganization energies[26-27] for electron transfer and concerted PCET to enable the calculation of free energy barriers and rate constants. The calculation of PCET rate constants also requires the generation of reactant and product proton potential energy curves and the associated proton vibrational wavefunctions and overlap integrals, which is straightforward for both EPT and E2PT processes.[20]

**Designing Molecular Electrocatalysts with Non-Innocent Ligands**

A wide range of metalloporphyrins have been shown experimentally to evolve hydrogen in acidic solution at modest overpotentials. Of particular interest are the cobalt and nickel hangman metalloporphyrins, which are designed to have a carboxylic acid hanging over the metal center.[28-30] These types of hangman metalloporphyrins have been shown to evolve $H_2$ at less negative potentials than the corresponding metalloporphyrins without the hanging group in acetonitrile.[28] Initially the mechanism was thought to involve proton transfer from the hanging carboxylic acid to the metal center. However, calculations suggested an alternative mechanism in which the proton is transferred from the hanging carboxylic acid to the *meso* carbon of the porphyrin, producing a phlorin intermediate.[18-19] This mechanism is an example of ligand non-innocence, where a reducing electron localizes mainly on the porphyrin ring instead of the metal center, leading to ligand dearomatization and protonation.

Our initial computational study focused on cobalt hangman porphyrins.[18] In this case, we found that the phlorin intermediate is formed under weak acid conditions. As depicted in Figure 2A, the first reducing electron localizes on the cobalt, but the second reducing electron localizes on the porphyrin, leading to dearomatization and buckling of the porphyrin ligand. Three pieces of evidence supported the formation of the phlorin intermediate. First, the distance from the carboxylic acid proton to the *meso* carbon (2.69 Å) is significantly shorter than that distance to the metal center (4.33 Å), where the latter also corresponds to a local minimum rather than the global minimum (Figure 2B). Second, proton transfer is thermodynamically more favorable to the *meso* carbon than to the metal center by ~11 kcal/mol. Third, the free energy barrier for proton transfer from the carboxylic acid to the *meso* carbon (Figure 2C) was computed to be 9 kcal/mol, which is in agreement with the experimentally estimated barrier of 8 kcal/mol.[29] In addition, a thermodynamically favorable mechanism for $H_2$ production through the phlorin intermediate was determined computationally for weak acid conditions. Interestingly, this pathway does not involve the formation of a metal-hydride intermediate, but rather entails reprotonation of the carboxylate hanging group and the eventual generation of $H_2$ from this proton and the proton on the *meso* carbon.

We performed similar calculations to investigate nickel hangman porphyrins.[19] Under weak acid conditions, two reduction steps were found to produce Ni(I) and a ligand radical, followed by a PCET reaction involving intramolecular electron transfer from the nickel center to the porphyrin ligand coupled to intramolecular proton transfer from the carboxylic acid hanging group to the *meso* carbon to produce the phlorin intermediate. This PCET reaction could be concerted, leading directly to the phlorin intermediate, or sequential, involving intramolecular electron transfer followed by intramolecular proton transfer. In both cases, electron transfer from

the metal center to the porphyrin ligand leads to dearomatization, which allows proton transfer to the *meso* carbon. Under strong acid conditions, the phlorin intermediate is formed after a single reduction. Thermodynamically favorable pathways for $H_2$ production through the phlorin intermediate were found computationally for both weak and strong acid conditions.

Motivated by these computational studies, the Nocera group was able to isolate the phlorin intermediate using the weak acid phenol, which is strong enough to form the phlorin intermediate but not strong enough to generate $H_2$.[19] The phlorin intermediate was characterized with spectroelectrochemistry, showing that the phlorin signature peak appears only with an applied potential of −1.9 V vs $Fc^+/Fc$ in the presence of phenol (Figure 3A). The phlorin was also identified with cyclic voltammetry (CV) through the appearance of an additional peak at a slightly more negative potential, corresponding to reduction of the phlorin (Figure 3B). Finally, CV simulations were performed, assuming the mechanism predicted by theory with the calculated thermodynamic and kinetic quantities, supplemented by fitted parameters. These CV simulations were in agreement with the experimental catalytic peaks for both tosic and benzoic acid for nickel porphyrins with and without the carboxylic acid hanging group. These combined experimental data support the theoretical prediction of a phlorin intermediate, although the specific pathways for $H_2$ production are not fully resolved. Most importantly, these combined computational and experimental studies on metalloporphyrins highlight the importance of ligand non-innocence in terms of controlling the localization of both electrons and protons, as well as the coupling between them.

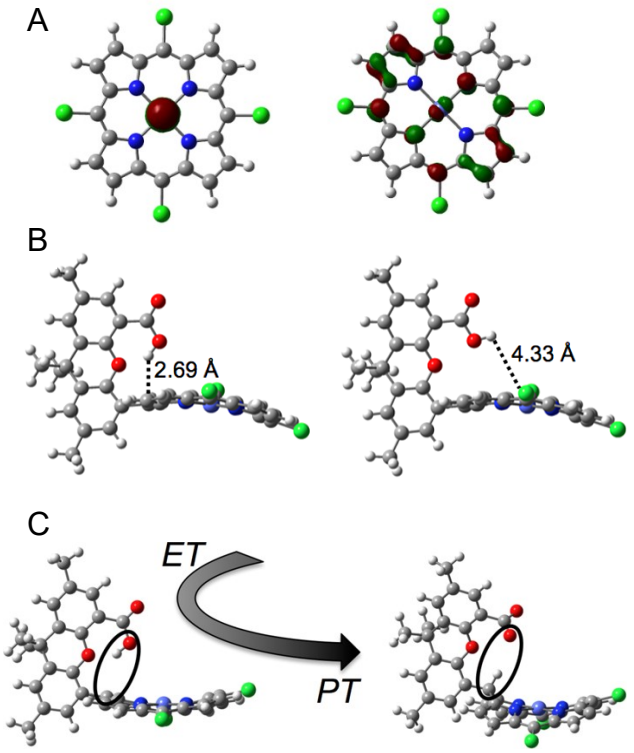


**Figure 2:** (A) Cobalt porphyrin without the hanging group, depicting the highest occupied molecular orbital after one reduction (left) and after two reductions (right), illustrating that the first reducing electron is localized on the cobalt, while the second reducing electron is mainly localized on the ligand. (B) Cobalt porphyrin with the carboxylic acid hanging group after two reductions, indicating that the proton transfer distance to the *meso* carbon (left, global minimum) is shorter than that to the cobalt (right, local minimum). The reaction free energy for proton transfer from the carboxylic acid is −11.6 kcal/mol to the *meso* carbon and −0.2 kcal/mol to the cobalt. (C) Illustration of proton transfer from the carboxylic acid to the *meso* carbon after the second reduction, producing the phlorin intermediate for the cobalt hangman porphyrin. The free energy barrier for this proton transfer was computed to be 9.0 kcal/mol. Adapted with permission from Ref. 18. Copyright 2014 American Chemical Society.

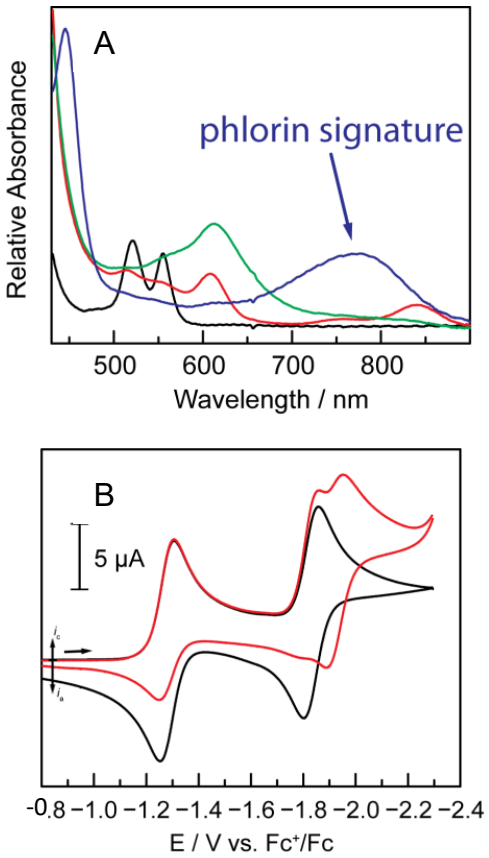


**Figure 3:** (A) Spectroelectrochemistry on the nickel porphyrin without a hanging group before electrolysis (black), at −1.3 V vs $Fc^{+}/Fc$ without acid (red), at −1.9 V vs $Fc^{+}/Fc$ without acid (green), and at −1.9 V with phenol (blue), highlighting the phlorin signature. (B) Cyclic voltammogram without acid (black) and with phenol (red), highlighting the additional peak corresponding to phlorin reduction. Adapted with permission from Ref. 19. Copyright 2016 US National Academy of Sciences.

**Designing Multi-Proton Relays**

A key reaction in solar energy conversion is the splitting of water into molecular hydrogen and oxygen. Photosystem II catalyzes this water splitting reaction starting with the oxidation of a Tyr residue, which transfers a proton to a neighboring His residue.[31-36] Artificial photosynthetic systems have been designed using this Tyr-His motif as inspiration.[4,36-37] Although it is not clear that this Tyr-His pair participates in a longer proton wire in Photosystem II,[38] many bioenergetic processes involve proton wires, where protons are transported over long distances through multi-

proton relays. Following nature's example, we have embarked upon combined experimental and computational studies aimed at designing multi-proton relay systems based on the Tyr-His motif.[20]

Initially the Moore groups designed a series of molecules in which the Tyr-His motif was represented by a benzimidazole phenol (BIP) molecule, with ester substituents serving as potential acceptors of the second proton. Our DFT calculations of the relative free energies of the PT states associated with the oxidized state indicated that the concerted mechanism, EPT, is favored for the BIP molecule without any substituents (Figure 4A). Moreover, the one-electron, one-proton transfer (EPT) mechanism was found to be more favorable than the one-electron two-proton transfer (E2PT) mechanism by ~14 kcal/mol for the BIP-$COOCH_3$ system (Figure 4B). For both systems, the experimentally measured and calculated redox potentials are ~1 V vs SCE in acetonitrile. Moreover, using our PCET theory, the kinetic isotope effect (KIE) was calculated to be ~2.0 for both systems, in agreement with the experimentally measured KIE of 1.8 for the BIP-$COOCH_3$ system (Table S1).

In an effort to theoretically design a multi-proton relay system, we investigated BIP molecules with amide and amino substituents.[20] On the basis of our calculations, we predicted that the molecules with amide substituents would still undergo EPT but that the molecules with amino substituents, including the BIP-$CH_2NEt_2$ system, would undergo E2PT (Figure 4C). These findings are consistent with the higher p$K_a$ values of the amino substituents, where the amine group serves as the proton acceptor, compared to those of the ester and amide substituents, where the carbonyl group serves as the proton acceptor. Furthermore, our calculations predicted that the E2PT process would shift the redox potentials to less positive potentials by ~300 mV. We also predicted that the KIE for the E2PT process in the BIP-$CH_2NEt_2$ system would be ~1.3, which is

lower than the KIEs of ~2.0 for the related EPT systems (Table S1). These KIEs are strongly influenced by contributions from excited electron-proton vibronic states.

Motivated by these predictions, the Moore group synthesized these four BIP systems and validated the theoretically predicted redox potentials and KIEs (Figure 5A, Table S1). Moreover, to verify the E2PT mechanism, the Moore group protonated the exocyclic amine of the BIP-$CH_2NEt_2$ system with trifluoroacetic acid (TFA), thereby blocking the second proton transfer, and found that the redox potential shifted back up to ~0.95 V vs SCE (Figure 5B). Spectroelectrochemistry experiments performed by the Kubiak group also confirmed the theoretically predicted EPT and E2PT mechanisms through spectral analysis of the products under an applied potential. While it is difficult to prove conclusively that the E2PT mechanism is fully concerted, the KIEs computed from the PCET theory under the assumption of a fully concerted mechanism are consistent with the experimental measurements. Moreover, CV simulations and DFT calculations of the free energy barriers suggested that an intermediate corresponding to EPT prior to the second PT would most likely be stable only on the ultrafast timescale, therefore resulting in an effectively concerted mechanism.[20]

This wide array of experiments validated our theoretical prediction that the redox potential will be ~1 V vs SCE for EPT and 0.6 – 0.7 V vs SCE for E2PT, while the KIE will be ~2 for EPT and ~1 for E2PT for these model systems. Given the complexity of PCET processes, these predicted trends are only valid for these specific types of model systems and are not generally applicable. For example, we found that the porphyrin-bound BIP molecule, which undergoes only EPT, exhibits a redox potential of ~1 V and a KIE of ~1 (Table S1). Analysis of the PCET calculations indicated that this lower KIE compared to the same unsubstituted BIP molecule without the porphyrin could be explained in terms of varying contributions from excited vibronic

states arising from the non-innocence of the porphyrin ligand following oxidation. This example illustrates that the KIE alone is not sufficient to assign a mechanism. These combined computational and experimental studies illustrate the predictive power of theory, as well as the ability to design multi-proton relays by tuning the p$K_a$ values and redox potentials. Future efforts will be aimed at using these design principles to produce E$N_p$PT systems with $N_p > 2$, which will involve $2^{N_p+1}$ diabatic states, as discussed above.

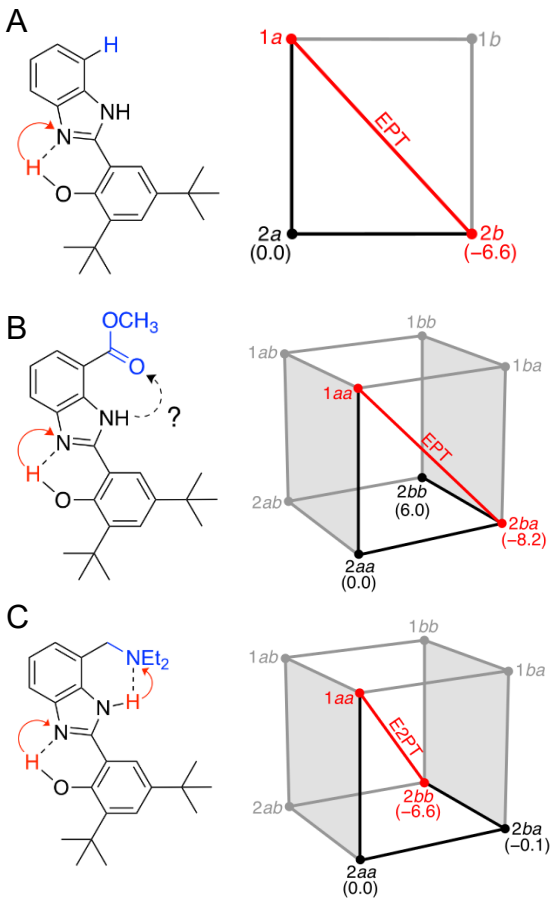


**Figure 4:** BIP molecules that exhibit PCET upon oxidation, where *1* and *2* denote the neutral and oxidized (cationic) state, and *a* and *b* denote the proton transfer state for the proton(s) that could potentially transfer. Relative free energies for the oxidized state are given in kcal/mol. (A) BIP-H, which is described in terms of four states, with EPT determined to be thermodynamically favorable; (B) $BIPCOOCH_3$, which is described in terms of eight states, with EPT determined to be thermodynamically favorable; (C) $BIP\text{-}CH_2NEt_2$, which is described in terms of eight states, with E2PT determined to be thermodynamically favorable. Adapted with permission from Ref. 20. Copyright 2017 American Chemical Society.

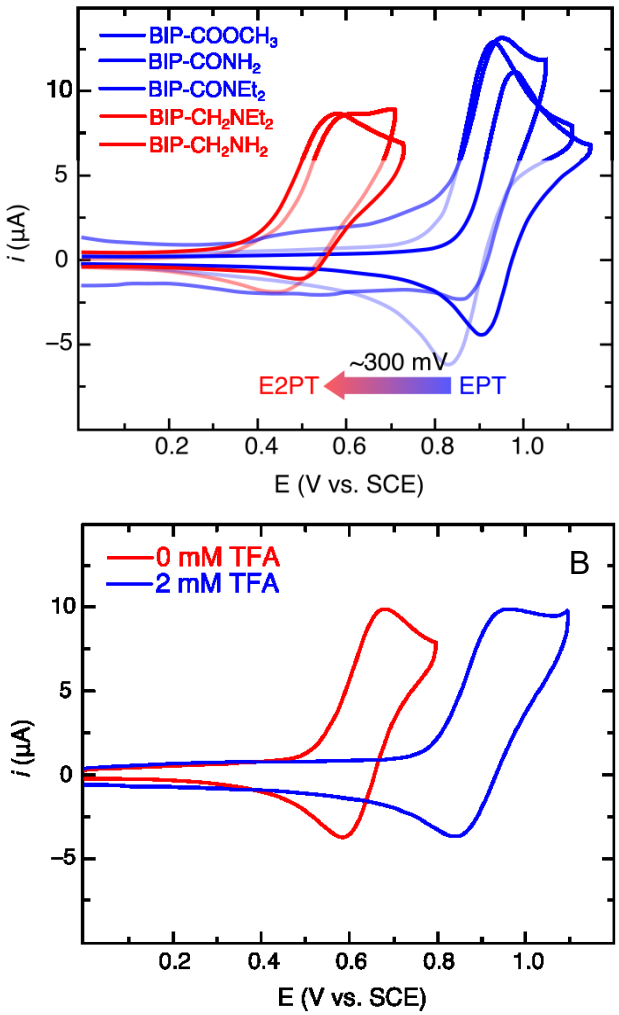


**Figure 5:** (A) CVs for the BIP systems indicated in the legend, including the ester that was initially studied experimentally and the four systems designed theoretically. The experimental data validate the theoretically predicted redox potentials for these four systems and clearly illustrate the predicted shift of ~300 mV for the E2PT process relative to the EPT process. (B) CVs for the BIP-$CH_2NEt_2$ system with and without TFA, which protonates the exocyclic amine and blocks the second proton transfer, thereby shifting the redox potential up to ~0.95 V vs SCE. These experimental data validate the theoretically predicted mechanism of E2PT for this system. Adapted with permission from Ref. 20. Copyright 2017 American Chemical Society.

**Designing Nanoparticles for Heterogeneous PCET**

The water splitting reaction has also been catalyzed photochemically using metal oxide nanoparticles. This type of photocatalytic water splitting reaction is typically described in terms of electrons and holes.[39-40] Recent experiments from the Mayer group,[41-42] however, have provided evidence that some of these interfacial redox reactions are actually PCET, involving protons as well as electrons. To investigate these types of interfacial PCET reactions, photoreduced colloidal ZnO nanocrystals (NCs) with dodecylamine capping groups in toluene were prepared by anaerobic ultraviolet irradiation to form electron/hole pairs, followed by quenching of the holes via oxidation of ethanol. After this procedure, the reducing electrons occupy delocalized orbitals in the conduction band, and the protons originating from the ethanol are thought to be located both on the surface and in the bulk of the NCs.

These photoreduced ZnO NCs react with the TEMPO radical through a PCET reaction to produce TEMPOH. Flash photolysis experiments were used to measure the second-order PCET rate constant to be ~$10^3$ $M^{-1}s^{-1}$.[41] The experimental data are consistent with a mechanism corresponding to a fast equilibrium associated with formation of a complex between the photoreduced ZnO NC and TEMPO radical, followed by PCET from the NC to TEMPO to produce TEMPOH:

$$\begin{array}{l} \mathrm{ZnO}:e_{\mathrm{CB}}^{-}/\mathrm{H}^{+}+\mathrm{TEMPO}\bullet \quad \cdots \quad \bullet \\ \left[\mathrm{ZnO}:e_{\mathrm{CB}}^{-}/\mathrm{H}^{+}\cdots \quad \bullet \quad \cdots \right. \end{array} \qquad (1)$$

Here $\mathrm{ZnO}:e_{\mathrm{CB}}^{-}/\mathrm{H}^{+}$ indicates the photoreduced ZnO NC with an electron in the conduction band and a proton on a surface oxygen. The second-order rate constant $k_2$ can be expressed as the product of an equilibrium constant $K_{\mathrm{eq}}$ associated with formation of the complex and the rate constant $k_{\mathrm{PCET}}$ for PCET within the complex:

$$k_2 = K_{\text{eq}} k_{\text{PCET}} \quad (2)$$

We used our PCET theory to investigate the process consisting of electron transfer from the conduction band of the ZnO NC to TEMPO concertedly with PT from a surface oxygen of the NC to the oxygen of TEMPO.[21] The input quantities to the rate constant expression, including the inner-sphere reorganization energy, the intrinsic energy difference, the proton potential energy curve parameters, and the electronic couplings, were computed with periodic DFT for the model shown in Figure 6. The ZnO reactive surface was assumed to be the non-polar $10\bar{1}0$ surface, represented as a periodic slab, because the removal of a hydrogen atom is expected to be thermodynamically more favorable for the non-polar surface than for the polar surface. Periodic DFT calculations of these types of systems are challenging, and hybrid functionals were required to obtain even qualitatively reasonable energetics, such as the exothermicity of the overall PCET reaction. Utilizing a partitioning scheme for computing electronic couplings, the highest occupied molecular orbital for $\text{ZnO}:e^-_{\text{CB}}$ hydrogen bonded to $TEMPOH^+$ was found to be delocalized over the entire slab, with somewhat greater localization on the hydrogen-bonding oxygen, for an approximate transition state geometry. The dependence of the vibronic couplings on the proton donor-acceptor (oxygen-oxygen) distance was included in this treatment, and the proton tunneling at the interface was gated by the low-frequency oxygen-oxygen motion. The calculated PCET rate constant of 2.5 x $10^3$ $s^{-1}$ is consistent with the experimentally measured second-order rate constant assuming an equilibrium constant of ~1 $M^{-1}$, which was determined to be consistent with the experimental data.[21]

The Mayer group also performed stopped-flow kinetics experiments to monitor the decay of the absorbance reflecting the concentration of electrons in the conduction band of the NC.[42] Although pseudo-first-order kinetics was expected for this process due to an excess of TEMPO,

the experimentally measured absorbance exhibited nonexponential decay kinetics. We performed kinetic Monte Carlo calculations[22] to determine if this experimental observation could be explained by proton diffusion in conjunction with PCET, which is assumed to be much faster than the diffusion process. First we identified the most stable hydrogen interstitial sites, also denoted proton sites, near the surface and inside the bulk with periodic DFT, employing slab models of the ZnO surface and three-dimensional models of bulk wurtzite crystal, respectively. Within these models, we calculated the barriers for proton hopping between different types of sites and estimated the associated rate constants. Subsequently, we generated a ZnO NC from bulk wurtzite crystal and categorized the stable proton sites based on the surface and bulk calculations.

To simulate the proton diffusion process depicted in Figure 7, we plugged all of these data into a kinetic Monte Carlo scheme, assuming that ~30% of the surface sites are inaccessible due to a proton bound to an oxygen site on the surface of the NC. This assumption is consistent with the concentration of capping ligands attached to zinc sites that could prevent PCET to TEMPO due to steric blocking, resulting in some protons remaining bound to the outer surface. Thus, the diffusing proton can be temporarily trapped in a subsurface site that is connected to a surface site already occupied by a bound proton. This trapped proton must diffuse to a different subsurface site that provides access to an unoccupied surface site prior to PCET. This situation leads to a broad distribution of survival probabilities with some longer lifetimes, resulting in nonexponential kinetics.

The survival probability calculated from our kinetic Monte Carlo simulations is consistent with the experimentally measured nonexponential decay of the absorbance. These simulations suggest that the nonexponential kinetics is due to proton diffusion within the bulk in conjunction with different types of subsurface and surface sites. These combined experimental and

computational studies highlight the importance of protons in photocatalysis at heterogeneous nanoparticle interfaces. The design of effective nanoparticle catalysts should consider the important roles of proton diffusion through the bulk and PCET at the surface, with special attention paid to the impact of capping ligands.

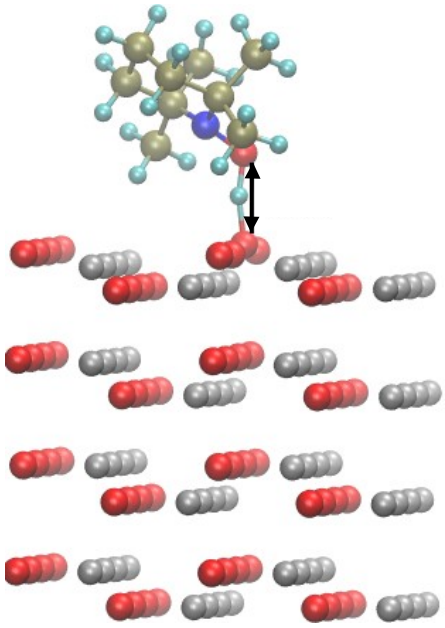

**Figure 6:** Model for PCET from the photoreduced ZnO NC to the TEMPO radical in toluene. The electron transfers from the conduction band of the NC to TEMPO concertedly with PT from a surface oxygen of the NC to the oxygen of TEMPO, producing TEMPOH. The proton donor-acceptor distance is indicated by a double-headed black arrow. Adapted with permission from Ref. 21. Copyright 2017 American Chemical Society.

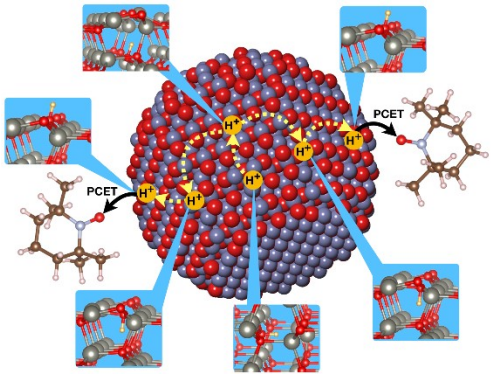


**Figure 7:** Schematic depiction of proton diffusion within the bulk of a photoreduced ZnO NC prior to reaching the surface, at which point it undergoes PCET to TEMPO. Adapted with permission from Ref. 22. Copyright 2017 American Chemical Society.

## Concluding Remarks and Outlook

Controlling the movement and coupling of electrons and protons is essential in the design of more effective catalysts for energy conversion processes. In the field of molecular electrocatalysis, the judicious use of non-innocent ligands provides the ability to localize electrons and protons on either the metal center or the ligand and to direct their motions accordingly. Incorporating multi-proton relays into molecular electrocatalysts enables the transport of protons over longer distances along preordained pathways, as well as the tuning of redox potentials through this movement of positive charge. Theoretical calculations are playing an important role in predicting the effects of different substituents, ligands, and metal centers on the thermodynamics, kinetics, and mechanisms of molecular electrocatalysts. The feedback between theory and experiment is critical to test and validate the theoretical predictions and drive the methodological developments toward experimentally accessible systems. As a result of this feedback, collaborative studies between experiment and theory are assisting in the design of more effective catalysts.

Although molecular electrocatalysts provide a significant degree of flexibility and diversity, the design of nanoparticle catalysts opens up new capabilities. The structure and size of nanoparticles, as well as the type and coverage of the capping ligands, determine their catalytic properties. The incorporation of protons into the bulk and on the surface of the nanoparticles allows the coupling of these protons with the electrons and holes that are involved in photocatalysis. Heterogeneous catalysis at the interface between the nanoparticle and the solvent provides opportunities for more diverse chemistry encompassing a combination of surface atoms and solvated molecules. Theoretical studies of heterogeneous catalysts encounter significant challenges because the systems are often not well-characterized experimentally and are more

difficult to describe computationally because of complications such as interfacial effects and defects. Thus, theoretical methods for heterogeneous catalysis are not as accurate or generally applicable as those for molecular electrocatalysts and have not yet attained the same level of predictive capability. Nevertheless, current developments in both theoretical and experimental methods for studying nanoparticles are leading to greater insights about their catalytic properties. A combination of molecular and heterogeneous catalysis may be the most effective approach for developing renewable energy sources to address the current energy challenges.

**Biographical Information**

Sharon Hammes-Schiffer received her B.A. in Chemistry from Princeton University in 1988 and her Ph.D. in Chemistry from Stanford University in 1993, followed by two years as a postdoctoral researcher at AT&T Bell Laboratories. She is currently the John Gamble Kirkwood Professor of Chemistry at Yale University.

**Acknowledgments**

I am grateful to the past group members who performed the calculations, drove the science, and created the figures: Brian Solis for the hangman metalloporphyrin project, Mioy Huynh for the multi-proton relay project, and Soumya Ghosh and Alexander Soudackov for the ZnO NC project. I am also grateful to our outstanding experimental collaborators, with special thanks to Dan Nocera, Ana Moore, Tom Moore, and Jim Mayer.

**Supporting Information.** Table of experimental and calculated redox potentials and KIEs for BIP molecules.

**Funding**

This work was supported by the NSF Grant CHE-13-61293 (PCET theory) and the Center for Chemical Innovation of the NSF (Solar Fuels, grant no. CHE-1305124, metalloporphyrins), as well as the Center for Molecular Electrocatalysis (multi-proton relays) and the Argonne-Northwestern Solar Energy Research (ANSER) Center (ZnO NCs), which are both Energy Frontier Research Centers funded by the U.S. Department of Energy, Office of Science, Office of Basic Energy Sciences.

**References**

(1) Alstrum-Acevedo, J. H.; Brennaman, M. K.; Meyer, T. J. Chemical Approaches to Artificial Photosynthesis. *Inorg. Chem.* **2005,** *44*, 6802-6827.
(2) Gust, D.; Moore, T. A.; Moore, A. L. Solar Fuels Via Artificial Photosynthesis. *Acc. Chem. Res.* **2009,** *42*, 1890-1898.
(3) Magnuson, A.; Anderlund, M.; Johansson, O.; Lindblad, P.; Lomoth, R.; Polivka, T.; Ott, S.; Stensjö, K.; Styring, S.; Sundström, V.; Hammarström, L. Biomimetic and Microbial Approaches to Solar Fuel Generation. *Acc. Chem. Res.* **2009,** *42*, 1899-1909.
(4) Zhao, Y.; Swierk, J. R.; Megiatto, J. D.; Sherman, b.; Youngblood, W. J.; Qin, D.; Lentz, D. M.; Moore, A. L.; Moore, T. A.; Gust, D.; Mallouk, T. E. Improving the Efficiency of Water Splitting in Dye-Sensitized Solar Cells by Using a Biomimetic Electron Transfer Mediator. *Proc. Natl. Acad. Sci. U.S.A.* **2012,** *109*, 15612-15616.
(5) Faunce, T.; Styring, S.; Wasielewski, M. R.; Brudvig, G. W.; Rutherford, A. W.; Messinger, J.; Lee, A. F.; Hill, C. L.; deGroot, H.; Fontecave, M.; MacFarlane, D. R.; Hankamer, B.; Nocera, D. G.; Tiede, D. M.; Dau, H.; Hillier, W.; Wang, L.-P.; Amal, R. Artificial Photosynthesis as a Frontier Technology for Energy Sustainability. *Energy Environ. Sci.* **2013,** *6*, 1074-1076.
(6) Hammes-Schiffer, S. Theoretical Perspectives on Proton-Coupled Electron Transfer Reactions. *Acc. Chem. Res.* **2001,** *34*, 273-281.
(7) Stubbe, J.; Nocera, D. G.; Yee, C. S.; Chang, M. C. Y. Radical Initiation in the Class I Ribonucleotide Reductase: Long-Range Proton-Coupled Electron Transfer? *Chem. Rev.* **2003,** *103*, 2167-2202.
(8) Huynh, M. H. V.; Meyer, T. J. Proton-Coupled Electron Transfer. *Chem. Rev.* **2007,** *107*, 5004-5064.
(9) Hammes-Schiffer, S.; Soudackov, A. V. Proton-Coupled Electron Transfer in Solution, Proteins, and Electrochemistry. *J. Phys. Chem. B* **2008,** *112*, 14108-14123.
(10) Hammes-Schiffer, S.; Stuchebrukhov, A. A. Theory of Coupled Electron and Proton Transfer Reactions. *Chem. Rev.* **2010,** *110*, 6939-6960.
(11) Warren, J. J.; Tronic, T. A.; Mayer, J. M. Thermochemistry of Proton-Coupled Electron Transfer Reagents and Its Implications. *Chem. Rev.* **2010,** *110*, 6961-7001.
(12) Hammes-Schiffer, S. Proton-Coupled Electron Transfer: Moving Together and Charging Forward. *J. Am. Chem. Soc.* **2015,** *137*, 8860-8871.

(13) Lennox, J. C.; Kurtz, D. A.; Huang, T.; Dempsey, J. L. Excited-State Proton-Coupled Electron Transfer: Different Avenues for Promoting Proton/Electron Movement with Solar Photons. *ACS Energy Lett.* **2017,** *2*, 1246-1256.
(14) Soudackov, A.; Hammes-Schiffer, S. Multistate Continuum Theory for Multiple Charge Transfer Reactions in Solution. *J. Chem. Phys.* **1999,** *111*, 4672-4687.
(15) Soudackov, A.; Hammes-Schiffer, S. Derivation of Rate Expressions for Nonadiabatic Proton-Coupled Electron Transfer Reactions in Solution. *J. Chem. Phys.* **2000,** *113*, 2385-2396.
(16) Soudackov, A.; Hatcher, E.; Hammes-Schiffer, S. Quantum and Dynamical Effects of Proton Donor-Acceptor Vibrational Motion in Nonadiabatic Proton-Coupled Electron Transfer Reactions. *J. Chem. Phys.* **2005,** *122*, 014505.
(17) Hammes-Schiffer, S. Proton-Coupled Electron Transfer: Classification Scheme and Guide to Theoretical Methods. *Energy Environ. Sci.* **2012,** *5*, 7696-7703.
(18) Solis, B. H.; Maher, A. G.; Honda, T.; Powers, D. C.; Nocera, D. G.; Hammes-Schiffer, S. Theoretical Analysis of Cobalt Hangman Porphyrins: Ligand Dearomatization and Mechanistic Implications for Hydrogen Evolution. *ACS Catal.* **2014,** *4*, 4516-4526.
(19) Solis, B. H.; Maher, A. G.; Dogutan, D. K.; Nocera, D. G.; Hammes-Schiffer, S. Nickel Phlorin Intermediate Formed by Proton-Coupled Electron Transfer in Hydrogen Evolution Mechanism. *Proc. Natl. Acad. Sci. U.S.A.* **2016,** *113*, 485-492.
(20) Huynh, M. T.; Mora, S. J.; Villalba, M.; Tejeda-Ferrari, M. E.; Liddell, P. A.; Cherry, B. R.; Teillout, A.-L.; Machan, C. W.; Kubiak, C. P.; Gust, D. Concerted One-Electron Two-Proton Transfer Processes in Models Inspired by the Tyr-His Couple of Photosystem II. *ACS Cent. Sci.* **2017,** *3*, 372-380.
(21) Ghosh, S.; Castillo-Lora, J.; Soudackov, A. V.; Mayer, J. M.; Hammes-Schiffer, S. Theoretical Insights into Proton-Coupled Electron Transfer from a Photoreduced ZnO Nanocrystal to an Organic Radical. *Nano Lett.* **2017,** *17*, 5762-5767.
(22) Ghosh, S.; Soudackov, A. V.; Hammes-Schiffer, S. Role of Proton Diffusion in the Nonexponential Kinetics of Proton-Coupled Electron Transfer from Photoreduced Zno Nanocrystals. *ACS Nano* **2017,** *11*, 10295-10302.
(23) Marcus, R. A.; Sutin, N. Electron Transfers in Chemistry and Biology. *Biochim. Biophys. Acta* **1985,** *811*, 265-322.
(24) Soudackov, A. V.; Hammes-Schiffer, S. Nonadiabatic Rate Constants for Proton Transfer and Proton-Coupled Electron Transfer Reactions in Solution: Effects of Quadratic Term in the Vibronic Coupling Expansion. *J. Chem. Phys.* **2015,** *143*, 11B613_1.
(25) Solis, B. H.; Hammes-Schiffer, S. Proton-Coupled Electron Transfer in Molecular Electrocatalysis: Theoretical Methods and Design Principles. *Inorg. Chem.* **2014,** *53*, 6427-6443.
(26) Ghosh, S.; Horvath, S.; Soudackov, A. V.; Hammes-Schiffer, S. Electrochemical Solvent Reorganization Energies in the Framework of the Polarizable Continuum Model. *J. Chem. Theory Comput.* **2014,** *10*, 2091-2102.
(27) Ghosh, S.; Soudackov, A. V.; Hammes-Schiffer, S. Electrochemical Electron Transfer and Proton-Coupled Electron Transfer: Effects of Double Layer and Ionic Environment on Solvent Reorganization Energies. *J. Chem. Theory Comput.* **2016,** *12*, 2917-2925.
(28) Lee, C. H.; Dogutan, D. K.; Nocera, D. G. Hydrogen Generation by Hangman Metalloporphyrins. *J. Am. Chem. Soc.* **2011,** *133*, 8775-8777.
(29) Roubelakis, M. M.; Bediako, D. K.; Dogutan, D. K.; Nocera, D. G. Proton-Coupled Electron Transfer Kinetics for the Hydrogen Evolution Reaction of Hangman Porphyrins. *Energy Environ. Sci.* **2012,** *5*, 7737-7740.

(30) Bediako, D. K.; Solis, B. H.; Dogutan, D. K.; Roubelakis, M. M.; Maher, A. G.; Lee, C. H.; Chambers, M. B.; Hammes-Schiffer, S.; Nocera, D. G. Role of Pendant Proton Relays and Proton-Coupled Electron Transfer on the Hydrogen Evolution Reaction by Nickel Hangman Porphyrins. *Proc. Natl. Acad. Sci. U.S.A.* **2014,** *111*, 15001-15006.
(31) Tommos, C.; Babcock, G. T. Proton and Hydrogen Currents in Photosynthetic Water Oxidation. *Biochim. Biophys. Acta* **2000,** *1458*, 199-219.
(32) Kuhne, H.; Brudvig, G. W. Proton-Coupled Electron Transfer Involving Tyrosine Z in Photosystem II. *J. Phys. Chem. B* **2002,** *106*, 8189-8196.
(33) Faller, P.; Goussias, C.; Rutherford, A. W.; Un, S. Resolving Intermediates in Biological Proton-Coupled Electron Transfer: A Tyrosyl Radical Prior to Proton Movement. *Proc. Natl. Acad. Sci. U.S.A.* **2003,** *100*, 8732-8735.
(34) Keough, J. M.; Jenson, D. L.; Zuniga, A. N.; Barry, B. A. Proton Coupled Electron Transfer and Redox-Active Tyrosine Z in the Photosynthetic Oxygen-Evolving Complex. *J. Am. Chem. Soc.* **2011,** *133*, 11084-11087.
(35) Hammarström, L.; Styring, S. Proton-Coupled Electron Transfer of Tyrosines in Photosystem II and Model Systems for Artificial Photosynthesis: The Role of a Redox-Active Link between Catalyst and Photosensitizer. *Energy Environ. Sci.* **2011,** *4*, 2379-2388.
(36) Megiatto Jr, J. D.; Méndez-Hernández, D. D.; Tejeda-Ferrari, M. E.; Teillout, A.-L.; Llansola-Portolés, M. J.; Kodis, G.; Poluektov, O. G.; Rajh, T.; Mujica, V.; Groy, T. L. A Bioinspired Redox Relay That Mimics Radical Interactions of the Tyr–His Pairs of Photosystem II. *Nat. Chem.* **2014,** *6*, 1862.
(37) Moore, G. F.; Hambourger, M.; Gervaldo, M.; Poluektov, O. G.; Rajh, T.; Gust, D.; Moore, T. A.; Moore, A. L. A Bioinspired Construct That Mimics the Proton Coupled Electron Transfer between P680•+ and the Tyrz-His190 Pair of Photosystem II. *J. Am. Chem. Soc.* **2008,** *130*, 10466-10467.
(38) Umena, Y.; Kawakami, K.; Shen, J.-R.; Kamiya, N. Crystal Structure of Oxygen-Evolving Photosystem II at a Resolution of 1.9 Å. *Nature* **2011,** *473*, 55.
(39) Maeda, K.; Domen, K. Photocatalytic Water Splitting: Recent Progress and Future Challenges. *J. Phys. Chem. Lett.* **2010,** *1*, 2655-2661.
(40) Akimov, A. V.; Neukirch, A. J.; Prezhdo, O. V. Theoretical Insights into Photoinduced Charge Transfer and Catalysis at Oxide Interfaces. *Chem. Rev.* **2013,** *113*, 4496-4565.
(41) Schrauben, J. N.; Hayoun, R.; Valdez, C. N.; Braten, M.; Fridley, L.; Mayer, J. M. Titanium and Zinc Oxide Nanoparticles Are Proton-Coupled Electron Transfer Agents. *Science* **2012,** *336*, 1298-1301.
(42) Braten, M. N.; Gamelin, D. R.; Mayer, J. M. Reaction Dynamics of Proton-Coupled Electron Transfer from Reduced Zno Nanocrystals. *ACS Nano* **2015,** *9*, 10258-10267.